MUON ENERGY LOSS IN LIQUID ARGON

KEVIN INGLES, UNIVERSITY OF SOUTH ALABAMA
THOMAS JUNK, FERMILAB
ALBERTO MARCHIONNI, FERMILAB

FERMILAB: SIST PROGRAM

Abstract. The DUNE Far Detector is a Liquid-Argon TPC that resides at the 4850 ft level at the Sanford Underground Research Facility. This detector allows for both the visualization and the measurement of charged particle energy deposition. Cosmic-rays that penetrate down to the detector have a wide energy range. Of focus in this study is 0.2 GeV to 1000 GeV. The detector response to the μ's is simulated using GEANT4. Mean energy loss and most probable energy loss are presented as a function of momentum. Preliminary results are given that will help develop and algorithm that determine energies from energy deposition of high-energy μ's.

Contents

1. Introduction

1.1. Bethe-Bloch Equation. As fast, $v = \beta c$, charged particles travel through matter they interact with it. These interactions include ionization and excitation at moderate energies. The Bethe-Bloch equation gives the expected energy loss for charged particles heavier than electrons travelling through a material. The formula can be written as

$$\left\langle -\frac{dE}{dx} \right\rangle = Kz^2 \frac{Z}{A} \frac{1}{\beta^2} \left[\frac{1}{2} \ln \frac{2m_e c^2 \beta^2 \gamma^2 W_{max}}{I^2} - \beta^2 - \frac{\delta(\beta\gamma)}{2} \right], \tag{1}$$

where $K = 0.307075$ MeV cm^2 mol^{-1} is a constant, z is the charge number ($Q = ze$), Z is the atomic number of the material, A is the atomic mass of the material in g mol^{-1}, hence $\langle -dE/dx \rangle$ has units MeV cm^2 g^{-1}, and I is the mean excitation energy obtained by summing the oscillation strengths of the atom *(add ref)*. The W_{max} factor is the maximum kinetic energy transferred to an electron in a single collision and expressed as *(add ref)*

$$W_{max} = \frac{2m_e c^2 \beta^2 \gamma^2}{1 + 2m_e/M\gamma + (m_e/M)^2}. \tag{2}$$

M denotes the mass of the incident particle. For high energies Eq. 2 grows as γ and results in the incident particle having potentially hard collisions. The δ factor in Eq. 1 is the density correction and describes how the expanding electric field of a fast charged particle is truncated due to polarization of the material, thus limiting how much energy can be lost. At very high energies

$$\frac{\delta}{2} = \ln \frac{\hbar\omega_p}{I} + \ln \beta\gamma + \frac{1}{2}. \tag{3}$$

Where $\hbar\omega_p$ is the plasma energy of the material. The density correction as parameterized by Sternheimer *(add ref)* is

$$\delta(\beta\gamma) = \begin{cases} 2(\ln 10)y - \overline{C} & \text{if } y \geq y_1 \\ 2(\ln 10)y - \overline{C} + a(y_1 - y)^k & \text{if} y_0 \leq y < y_1. \\ 0 & \text{if} y < y_0 (\text{nonconductors}) \end{cases} \tag{4}$$

Here $y = log_{10}\beta\gamma$, $\overline{C}$ is obtained equation Eq. 3 with Eq. 4, and y_0, y_1, a and k are fitted parameters. To write $\langle -dE/dx \rangle$ as a function of momentum let $\beta\gamma = p/M$, $\beta^2 = [(M/p)^2 + 1]^{-1}$ and $\gamma^2 = (p/M)^2 + 1$.

For very high energy particles the expected energy loss is given by

$$\left\langle -\frac{dE}{dx} \right\rangle = a(E) + b(E)E, \tag{5}$$

here $a(E)$ is given by Eq. 1 and $b(E)$ is a very slowly varying function that accounts for the radiative losses. The function $b(E)$ can be split up into three pieces

$$b_{tot} = b_{brems} + b_{pair} + b_{nucl} \tag{6}$$

where the components account for bremsstrahlung, direct paired production and nuclear interaction. Direct paired production differs from conventional paired production insofar as instead of having photons convert, the positron-electron pair is created directly from the charged particle. An example of the of Eq.1, 5, 6 for μ's in liquid argon can be seen in Fig. 1.

1.2. Landau Distributions: Most Probable Value. From Eq. 1 one obtains the expected value of energy loss, which is weighted by rare and hard collision. The Landau-Vavilov distribution describes the energy loss of a single particle with a specific momentum. The Landau-Vavilov distribution is given as an integral *(add ref)*

$$\frac{P(\lambda)}{\xi} = \frac{1}{2\pi i \xi} \int_{c-i\infty}^{c+i\infty} e^{s \log s + \lambda s} ds \tag{7}$$

The integral must be evaluated numerically. The factor ξ

$$\xi = \frac{1}{2} K z^2 \frac{Z}{A} \frac{x}{\beta^2} \tag{8}$$

is momentum dependent, x is units g cm^{-2} and λ is given by

$$\lambda = \frac{1}{\xi}(\Delta_p - \langle \Delta \rangle) - \beta^2 - \ln \frac{\xi}{W_{max}} - 1 + \Gamma_E \tag{9}$$

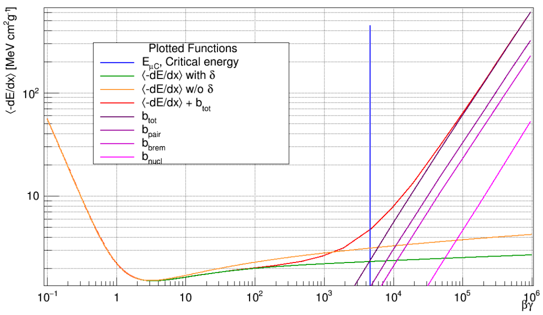

FIGURE 1. Expected energy lossfor μ's in liquid Argon

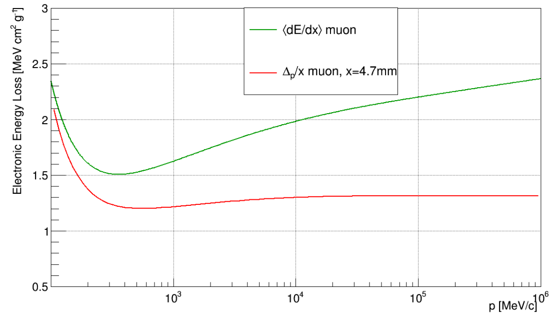

FIGURE 2. Bethe-Bloch and Landau-Vavilov-Bichsel compared

Here ξ and W_{max} are given by their previous definitions and Γ_E is Euler's constant. The Δ_p is most probable energy loss value (MPV) and $\langle\Delta\rangle$ is the expected energy loss respectively.

The MPV sits at the top of the Landau-Vavilov distribution. How this value changes with momentum is given by the Landau-Vavilov-Bichsel (LVB) equation *(add ref)*

$$\Delta_p = \xi \left[\ln \frac{2m_e c^2 \beta^2 \gamma^2}{I} + \ln \frac{\xi}{I} + j - \beta^2 - \delta(\beta\gamma) \right] \tag{10}$$

This expression has plateau at high energies known as the "Fermi Plateau" and given by

$$\Delta_p \underset{\beta\gamma \gtrsim 100}{\longrightarrow} \xi \left[\ln \frac{2mc^2 \xi}{(\hbar\omega_p)^2} + j \right]. \tag{11}$$

It is worth noting that the relativistic rise observed is due to W_{max}. See Fig. 2.

In Fig. 3 LArIAT used the LVB equation to tune their detectors calibration constant, the data is seen to follow the slow growing track of the dotted red curve better than that of the solid red line (LVB and Bethe-Bloch, respectively). The calibration, when applied to the protons, then shows that the proton energy loss behavior follows that of LVB equation as well.

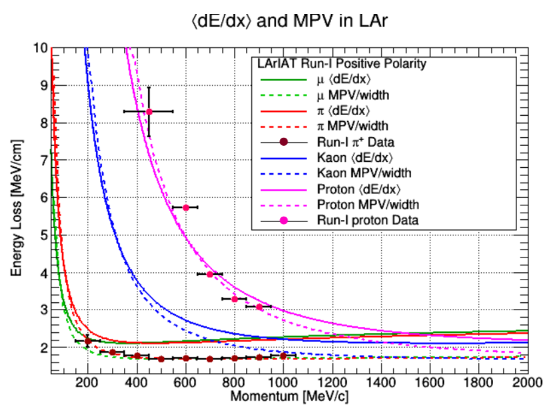

FIGURE 3. LArIAT tuning detector to my analytical curves.

1.3. **Knock-on electrons (δ rays).** Knock-on electrons, or delta rays, are electrons that have been freed from their atoms and can travel freely. For spin-$\frac{1}{2}$ particles the distribution of δ rays with $T_e \gg I$ is given by *(add ref)*

$$\frac{d^2N}{dTdx} = \frac{1}{2}Kz^2 \frac{Z}{A}\frac{1}{\beta^2}\frac{1}{T_e^2}\left[1 - \beta^2 \frac{T_e}{W_{max}} + \left(\frac{T_e}{T+m}\right)^2\right] \tag{12}$$

where T and m are the kinetic energy and rest mass of the incident particle. The expression in the brackets was obtained from Rossi *(add ref)*. Integrating this expression over $I \ll T_{cut} \le T_e \le W_{max}$ one obtains

$$\frac{dN}{dx} = \frac{1}{2} K z^2 \frac{Z}{A} \frac{1}{\beta^2} \left[\frac{1}{T_{cut}} - \frac{1}{W_{max}} + \zeta \ln \frac{T_{cut}}{W_{max}} + \frac{\xi}{2}(W_{max} - T_{cut}) \right]. \tag{13}$$

Here $\zeta = \beta^2/W_{max}$ and $\xi = 1/(T+m)^2$. Written in terms of momentum, the expression ξ simplifies to $\xi = 1/(p^2+m^2)$. In Fig. 4 the expressions above have been plotted for various momenta of incident μ's in liquid argon (LAr) and cut-off energies for knock-on electrons. The plots indicate that the production of energetic (> 1 MeV) δ rays is very weakly dependent on the incident particle's momentum.

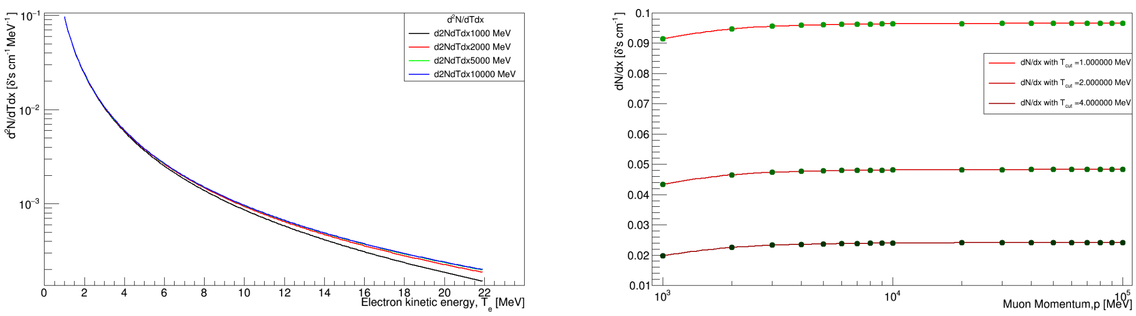

FIGURE 4. Left Eq. 12 with various μ momenta, and right Eq. 13 at various cut-off kinetic energies

2. Simulation and Analysis

2.1. The Detector. The detector geometry used was that of a single phase 10 kt module of the DUNE Far Detector. It's fiducial volume dimensions are 16x16x57 meters. The detector is split up into a top half and a bottom half. The detector contains 300 Time Projection Chambers(TPC). See Fig. 5 for the counting scheme. Each TPC has three sets of wires, two induction planes U and V and a collection plane Z. The induction plane are orientated to make 35° angles. Each TPC contains 960 Z plane wires and 800 induction plane wires each.

During simulation the LArSoft software package is responsible for drifting ionized charged towards the wire. The drift length is 3.6 m. To properly install the electronics for DUNE's Far Detector, the induction plane wires are wrapped around their frame, thus giving charge deposits the ability to hit the same wire twice.

The wire plane of interest is the collection plane. These wire are meant to do a calorimetric measurement if the drifted charge. The collection plane, oriented in the Z-direction, has a wire pitch 4.79 mm.

2.2. Simulation. There were approximately 12,000 simulated μ's total, at 12 different energies. These μ's were shot with a specific momentum and no spread in the All simulated particles started at the same exact spot: (100,100,10) centimeters, which equates to starting in TPC 9 a little inside the detector. For a 1 GeV μ the event display is given in Fig. 6.

The LArSoft software package is responsible for drifting the ionized charge to the wires. To get the full deposited energy from the μ to drift to the wires longitudinal and transverse diffusion and well as recombination were all turned off. In addition the electron lifetime was elongated. To get the energy loss as calculated by GEANT4 the steps onere set to include every voxel boundary crossing in the detector.

Simulations of moderate energy electrons (0.2 GeV to 1 GeV) averaged to have a peak memory usage of 1100 MB and lasted around 30 sec. However, the higher energy μ's, (> 10 GeV), which also made it through the entire detector, varied largely in the peak memory usage from 900 MB to 9000 MB and typically lasted 120 sec.

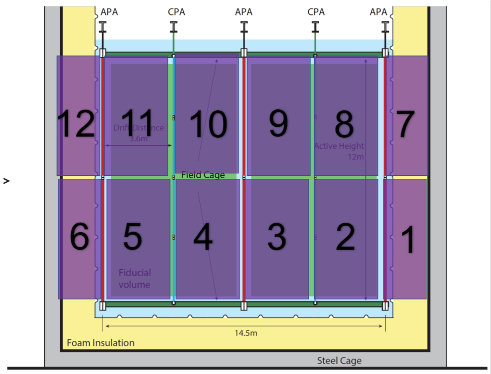

FIGURE 5. Orientation is from beam, how TPCs are counted in simulation

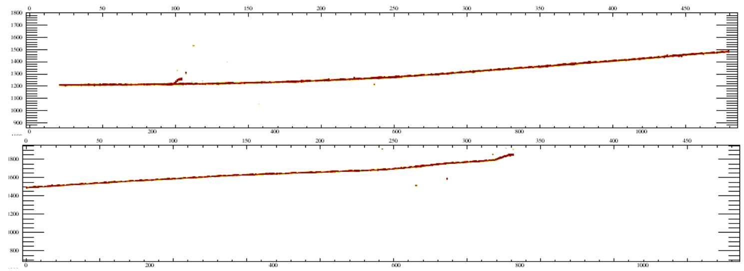

FIGURE 6. 1 GeV μ event display, the slope is due to Coloumb scattering

2.3. **Analysis.** The analysis was done using MCTruth from the MCParticles. In order to process the information, data from the ART files was packaged into an ntuple. Two ntuples were created, one that stored the energy deposition information and one that stored the energy loss information. The information for charge deposits on wires was stored in the sim::IDE data format and the data for the energy loss in the MCTrajectory points format. The analyis module used was dervied from the AnalysisExample_module.

2.3.1. *Energy Deposition.* For each wire, the charge deposited on the wire was summed up, converted to energy and divided by the μ track length as seen by that wire.To minimize the momentum loss, as to make the use of a Landau distribution fit most appropriate only the first twenty wires were chosen to fill a histogram. A fit was performed over two ranges, one the focused on fitting the maximum and one that focused on fitting the full-width half maximum. These two fits were made to reconcile the systematic error introduced in trying to fit a a Landau distribution to distribution that is not completely Landau distributed. The average of these two fits was used as the GEANT4 prediction and their difference as the systematic error.

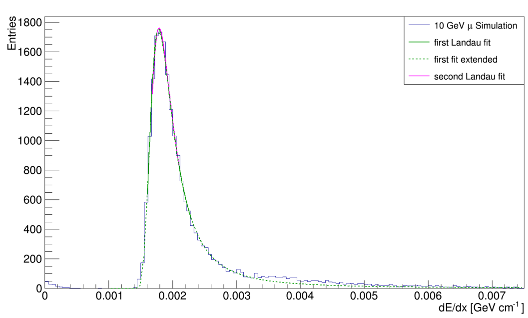

FIGURE 7. 10 GeV μ charge deposit distribution for first 20 wires

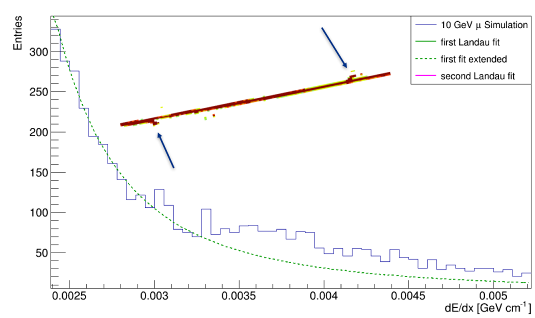

FIGURE 8. 10 GeV δ ray shoulder and muon track with δ rays present

To elaborate on why the energy deposition distribution are not perfectly Landau distribute note that the Landau distribution describes energy loss of a single μ with a specific momentum. However, even travelling two wires introduce a change in the μ momentum. Consequentially the histogrammed distribution is inherently non-Landau. Additionally, focusing on Fig. 8, due to energetic enough δ rays wires collect ionized charge from both the μ and the δ ray effectively doubling the energy deposition on that wire. This is what introduces the shoulder and the distortion from the Landau shape.

Since the μ losses energy as it travels the first 20 wires, it would be false to report the plotted momentum as the initial momentum. Instead, using 1 the average energy lost was found, multiplied by the distance traveled to and divided by 2 to get the *average* energy lost along the track of that wire. This was then

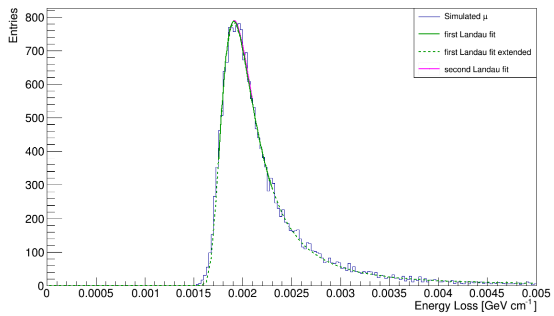

FIGURE 9. 200 MeV μ true energy loss in DUNE Far Detector

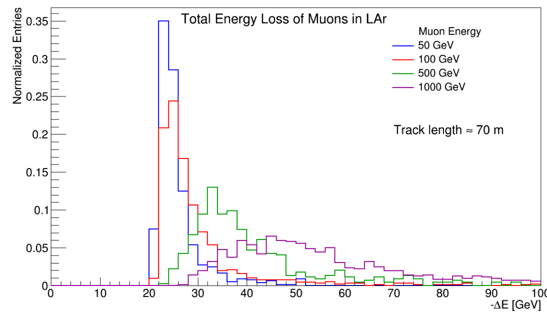

FIGURE 10. Total energy loss in DUNE Far Detector

subtracted from the initial momentum and the new value used as the plotted point. This method introduces an error of less than 1% as opposed to finding the energy using Einstein's equations.

2.3.2. *Energy Loss.* Another difference between the energy loss and energy deposition is the fact the the charge is drifted to the wires by the LArSoft software package for LAr detectors, whereas the energy loss is purely GEANT4. This means that LArSoft could introduce an error when finding MPV's from energy deposition distributions. GEANT4 simulates in steps where each step is recorded as the μ crossing a voxel boundary. Voxels have a side length of 30o microns. Taking scattering into consideration, the average amount of steps between two wires was taken to be 17. However, because slower particles scatter more, meaning the crossed voxel boundaries more often, their measure path was shorter than that of the faster particles. Therefore a analytical calculation was done for the given momentum shifted back as previously described. Note that this also introduces an error as the MPV of the average momentum is not the same as the average MPV of the momentum range. However, the introduced error is again less than 1%.

Again a histogram was filled for every 17 steps dividing the energy lost by the path length traveled. The same fits were performed, using two fits as opposed to one follows the reason described in Sec. 2.3.1. The average was again taken as the GEANT4 predicted value and the difference as the systematic error.

As expected this distribution does not have the δ ray shoulder as observed in the energy deposition distribution.

2.3.3. *Total Energy Loss.* A small study was done to look into the the energy loss distribution of moderately high-energy to high-energy μ's through out the entire detector. The moderately high-energy μ's still retain a sharp peak and a long tell reminiscent of a Landau distribution, but as the momentum increases the distribution smears out. This is do to the radiative losses. Which means that using energy deposition measurements to estimate incident μ energy is impractical as the big fluctuations in energy lost don't allow for good identification.

2.4. **Results.** Fig. 11 contains both analytically predicted and GEANT4 predicted values. The black points should be compared with, and the green points should be compared with the blue triangles. Both sets follow the LVB shape, however the GEANT4 predictions are consistently $\sim 2\%$ higher than the analytical predictions. Efforts were made to justify the discrepancy by comparing the values for variable used in GEANT4 and in the analytical formulas, however the change is adjusting to the same values gave a correction of less than 1%. This lead to trying to further understand the formulae. Specifically the Landau's constant term is of interest. Its derivation is ambiguous and literature states it's value has changed in the past.

3. CONCLUSION

An investigation into the agreement of the GEANT4 models with the analytical models was made. The simulation predicted values follow the shape of the analytical models but sits roughly 2% above it. This small different is not alarming and is even surprisingly good agreement, however the interest is in figuring out what has introduced this discrepancy. Some ideas include comparing GEANT4 predictions to other simulation software such as FLUKA or MARS15. Another approach might be to get the average form the

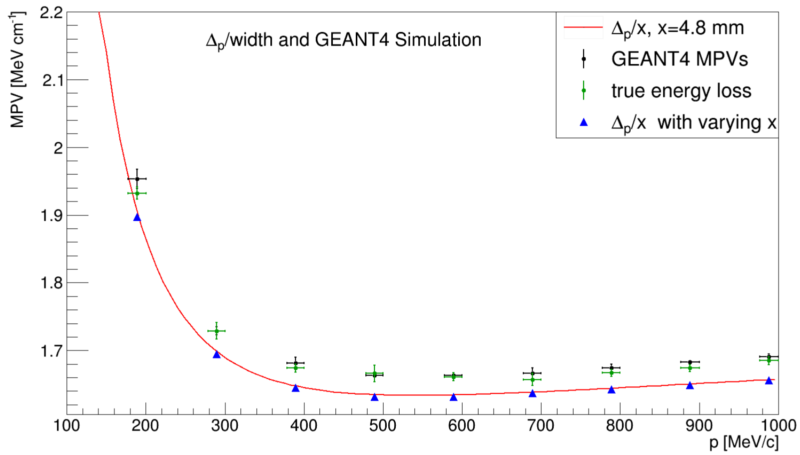

FIGURE 11. GEANT4 and analytical predictions compared from both energy deposition and energy loss

the energy deposition and loss distributions and comparing these to the Bethe-Bloch predict value. However the main course of action remains to resolve any possible bug in the simulation that could possible account for the 2% difference.

Since δ rays are fairly independent of the mu momentum and high-energy μ's have very large fluctations these to methods of determining μ are implausible. A literary search showed that ideas proposing to count the number of electromagnetic showers along a μ track might be a feasible method of approach.